

ISTITUTO NAZIONALE DI FISICA NUCLEARE
Laboratori Nazionali di Frascati

LNF-79/77(P)
17 Dicembre 1979

A. Majewski: MULTIPLE SCATTERING IN NUCLEUS-NUCLEUS
COLLISIONS AT MEDIUM AND HIGH ENERGIES.

A. Małecki^(x): MULTIPLE SCATTERING IN NUCLEUS-NUCLEUS COLLISIONS AT MEDIUM AND HIGH ENERGIES^(o).

ABSTRACT.

The Glauber model and the optical model of multiple scattering in collisions of complex nuclei have been discussed. The latter approach which is grounded upon the construction of the microscopic nucleus-nucleus potential can be considered as being an extrapolation of the former one towards lower energies. Various multiple-scattering expansions have been presented. Useful approximations, obtained by partially neglecting the intermediate excitations in the colliding nuclei, are considered.

1. - INTRODUCTION.

This lecture will be concerned with multiple scattering effects in the nucleus-nucleus collisions at medium and high energies. By medium energies we mean several hundred MeV/nucleon, by high energies - the ones of one order of magnitude greater.

Reactions with complex nuclei involve a very broad domain of problems and physical phenomena. Therefore, it will be instructive, at the beginning, to localize the position of our subject in this spacious area. Heavy ion scattering is characterized by three properties:

- i) short wave-length;
- ii) strong Coulomb interaction;
- iii) strong absorption.

It is convenient to refer to these three features as to the coordinates in a space of physical properties which characterize the collision of two nuclei.

Re i). At medium and high energies the wave lengths are short indeed. For heavy nuclei they are short even at relatively low energies. The short wavelengths justify the concept of classical trajectories⁽¹⁻⁴⁾, based on the Wentzel-Kramers-Brillouin (WKB) approximation to quantum scattering. At higher energies one may go further and use the eikonal approximation⁽⁵⁻⁷⁾ instead of

(x) Permanent address: Institute of Nuclear Physics, 31-342 Krakow (Poland).

(o) Lecture presented at the International School of Physics 'E. Fermi' on Nuclear Structure and Heavy Ion Collisions, Varenna, 9-21 July 1979.

WKB. In a classical language this would correspond to rectilinear trajectories. In fact, in energetic collisions most of the scattering occurs to a very forward direction. The eikonal approximation constitutes a basis for the microscopic Glauber model^(6, 8) of scattering between composite nuclei.

There is also another aspect of fast collisions. At sufficiently high energies one may neglect the energies of nuclear excitations with respect to the projectile energy. The former are of the order of 10 MeV. Thus at medium energies one there is at least one order of magnitude higher on the energy scale. The approximation of energetic degeneracy of nuclear states simplifies enormously the description of scattering. For example the third order contribution to elastic scattering amplitude in Watson's theory of multiple collision may be written as follows:

$$\sum_{j,k,l} \sum_{|n\rangle, |n'\rangle} \langle 0 | t_j | n \rangle G_n \langle n | t_k | n' \rangle G_{n'} \langle n' | t_l | 0 \rangle \approx \sum_{j,k,l} \langle 0 | t_j G_o^+ t_k G_o^+ t_l | 0 \rangle, \quad (1)$$

where we have neglected excitation energies E_n in scattering propagators:

$$G_n = (E - E_n + \frac{v^2}{2\mu} + i\epsilon)^{-1} \approx (E + \frac{v^2}{2\mu} + i\epsilon)^{-1} \equiv G_o, \quad (2)$$

and applied the relation of completeness:

$$\sum_n |n\rangle \langle n| = \sum_{n'} |n'\rangle \langle n'| = 1. \quad (3)$$

The "closure approximation"⁽⁹⁾ of Eq. (1) allows to avoid all the complications of coupled channels typical for low energy collisions, e. g. elastic scattering is independent of the structure of excited nuclear states. Eq. (1) is being often referred to as the "fixed scatterers" approximation. This corresponds to a picture of scattering where the projectile moves much faster than any signal of perturbation it can produce in the nuclear medium. The projectile sees the target nucleons as if they were frozen at fixed positions. Of course, various spatial configurations of nucleons are being averaged out with the aid of the ground state nuclear wave function $|0\rangle$.

Re ii). The strong Coulomb field can distort the incoming wave giving rise to the Fresnel effects in the elastic scattering⁽¹⁰⁾ angular distributions. However, in very energetic collisions the curvature of the projectile wave front over the target is negligible. That is why at medium and high energies the angular distributions are typical of Fraunhofer diffraction⁽¹⁰⁾, i. e. strongly forward-peaked and developing regular oscillations. One roughly has:

$$\frac{d\sigma}{d\Omega} \approx (kR^2)^2 \left[\frac{J_1(qR)}{qR} \right]^2 \Phi^2(q) \quad (4)$$

(k being initial momentum and q -momentum transfer), which corresponds to scattering by a perfectly absorbing sphere of radius R with a form factor $\Phi(q)$ accounting for the diffuseness of target. Due to this form factor the maxima in the Fraunhofer pattern are strongly depressed at larger angles. The Coulomb interaction has an important role in determining the depths of diffraction minima; of particular significance being its interplay with the real part of the nuclear scattering amplitude⁽¹¹⁾.

Re iii). Strong absorption means that colliding nuclei can easily be removed from the elastic channel by an excitation. This gives rise, via the unitarity, to diffraction which corresponds to the propagation of waves into classically forbidden or shadowed regions. At sufficiently high energy the elastic scattering is predominantly diffractive, i. e. it can be regarded as a shadow of a large number of inelastic processes. The inelasticity comes from two sources: excitation of nuclear states and inelasticity connected with the particle production in nucleon-nucleon collisions. The nuclear inelasticity may be treated by means of the closure approximation - see Eq. (1). The elastic scattering amplitude is thus calculated as a sum over all possible intermediate excitations of colliding nuclei. The elementary inelasticity is taken into account by utilizing the experimental nucleon-nucleon scattering amplitude; at medium and high energies they are main

ly imaginary. It can be observed that in our energy range the total N-N cross-sections are of the order of tens mb. At low energies they are greater-of the order of 1 b. Therefore two fast nuclei can penetrate each other during scattering to a greater extent than they do at lower energies.

In this lecture we shall discuss exclusively elastic scattering. Elastic collision of two nuclei does not represent a very spectacular event like nuclear fragmentation, shock waves or fireballs. However, it is of fundamental importance since the elastic channel contributes to any kind of collision and therefore deserved a particular attention.

2. - THE GLAUBER MODEL OF NUCLEUS-NUCLEUS SCATTERING.

In the eikonal approximation, that is believed to be valid at high energy and small scattering angles, the scattering amplitude at a momentum transfer q is written as:

$$F(q) = \frac{ik}{2\pi} \int d^2b e^{i\vec{q} \cdot \vec{b}} \left[1 - e^{i\chi(b)} \right], \quad (5)$$

where the eikonal phase-shift function is related to the potential of interaction V as follows:

$$\chi(b) = - \frac{1}{v} \int_{-\infty}^{+\infty} dz V(\sqrt{b^2 + z^2}), \quad (6)$$

k and v are the c.m. momentum and relative velocity, respectively. The plane of integration in Eq. (5) is referred to as the plane of impact parameter vectors. They are perpendicular to the average momentum (the bisectrix of the scattering angle) rather than to the initial momentum. This choice of the eikonal axis Oz allows to extend the angular range of validity of the approximation.

Suppose that the scattering potential is composed of the interactions between individual nucleons of the projectile and target nuclei:

$$V = \sum_{j=1}^A \sum_{k=1}^B V_{jk}(\vec{r} + \vec{r}_{jA} - \vec{r}_{kB}), \quad (7)$$

where $\vec{r}(\vec{b}, z)$ is the relative coordinate of the two nuclei, and $\vec{r}_{jA}(\vec{s}_{jA}, z_{jA})$, $\vec{r}_{kB}(\vec{z}_{kB}, z_{kB})$ denote the coordinates of the j -th nucleon of the projectile A and of the k -th nucleon of the target B , respectively. These are intrinsic nucleon coordinates, related to the centres-of-mass of the two nuclei.

From Eq. (7) follows additivity of individual phase-shifts:

$$\chi(b) = \sum_{j=1}^A \sum_{k=1}^B \chi_{jk}(\vec{b} + \vec{s}_{jA} - \vec{s}_{kB}). \quad (8)$$

The scattering amplitude can be therefore written:

$$F_{Gl}(q) = \frac{ik}{2\pi} \int d^2b e^{i\vec{q} \cdot \vec{b}} \left\{ 1 - \langle 0_A 0_B \left| \prod_{j=1}^A \prod_{k=1}^B \left[1 - \gamma_{jk}(\vec{b} + \vec{s}_{jA} - \vec{s}_{kB}) \right] \right| 0_A 0_B \rangle \right\} \quad (9)$$

where

$$\gamma_{jk} = 1 - e^{i\chi_{jk}}, \quad (10)$$

and the nuclear ground states $|0_A\rangle$, $|0_B\rangle$ have been inserted to average over all the configurations of bound nucleons.

The functions γ_{jk} , called the elementary profiles, are to be related to the nucleon-nucleon scattering amplitude:

$$f_{jk}(\delta) = \frac{ik}{2\pi} \int d^2b e^{i\delta \cdot \vec{b}} \gamma_{jk}(b), \quad (11)$$

and can be obtained from experiment with free nucleons by inverting Eq. (11).

The total nucleon-nucleon cross-section can be expressed in terms of the profile:

$$\sigma_{NN} = \frac{4\pi}{k} \text{Im} f(0) = 2 \int d^2b \text{Re} \gamma(b). \quad (12)$$

If the scattering amplitude is mostly imaginary then the profile $\gamma(b)$ is a real function and, on the ground of Eq. (12), it may be interpreted⁽⁸⁾ as the probability density of whichever interaction between nucleons colliding at the impact parameter b .

Using the rules of the probability calculus one obtains for two composite nuclei the following expression for the total profile:

$$\Gamma_{G1}(b) = 1 - \langle 0_A 0_B \left| \prod_{j=1}^A \prod_{k=1}^B \left[1 - \gamma_{jk}(\vec{b} + \vec{s}_{jA} - \vec{s}_{kB}) \right] \right| 0_A 0_B \rangle. \quad (13)$$

This is in a complete agreement with Eq. (9) since the nuclear profile $\Gamma_{G1}(b)$ should be the two-dimensional Fourier transform of the scattering amplitude $F_{G1}(q)$. Thus the eikonal approximation which gives rise to the additivity of phase-shifts is consistent with the probabilistic interpretation of the profile.

Eqs. (9) and (13) are referred to as the Glauber model of multiple scattering⁽⁶⁾. The model previously used for nuclear scattering of elementary hadrons⁽¹²⁾ has been generalized for nucleus-nucleus collisions firstly by Czyz and Maximon⁽⁸⁾.

By multiplying the AB factors in Eq. (9) or in Eq. (13) one obtains Glauber's series of multiple scattering:

$$F_{G1}(q) = F^{(1)} + F^{(2)} + F^{(3)} + \dots + F^{(AB)}, \quad (14)$$

$$\Gamma_{G1}(b) = \Gamma^{(1)} + \Gamma^{(2)} + \Gamma^{(3)} + \dots + \Gamma^{(AB)}, \quad (15)$$

where $F^{(n)}$ and $\Gamma^{(n)}$ denote the contributions of terms containing the product of n profiles γ ; for a given n there are $\binom{AB}{n}$ such terms. The series are finite and the successive contributions appear with alternative signs. To illustrate their structure let us write the first three contributions to the nuclear profile:

$$\Gamma^{(1)}(b) = AB \langle 0_A 0_B \left| \gamma(\vec{b} + \vec{s}_{1A} - \vec{s}_{1B}) \right| 0_A 0_B \rangle, \quad (16)$$

$$\Gamma^{(2)}(b) = - \left[2! \binom{A}{2} \binom{B}{2} \langle 0_A 0_B \left| \gamma(\vec{b} + \vec{s}_{1A} - \vec{s}_{1B}) \gamma(\vec{b} + \vec{s}_{2A} - \vec{s}_{2B}) \right| 0_A 0_B \rangle \right. \quad (17a)$$

$$\left. + \frac{1}{2} AB(B-1) \langle 0_A 0_B \left| \gamma(\vec{b} + \vec{s}_{1A} - \vec{s}_{1B}) \gamma(\vec{b} + \vec{s}_{1A} - \vec{s}_{2B}) \right| 0_A 0_B \rangle \right. \quad (17b)$$

$$\left. + \frac{1}{2} A(A-1)B \langle 0_A 0_B \left| \gamma(\vec{b} + \vec{s}_{1A} - \vec{s}_{1B}) \gamma(\vec{b} + \vec{s}_{2A} - \vec{s}_{1B}) \right| 0_A 0_B \rangle \right] \quad (17c)$$

$$\Gamma^{(3)}(b) = 3! \binom{A}{3} \binom{B}{3} \langle 0_A 0_B \left| \gamma(\vec{b} + \vec{s}_{1A} - \vec{s}_{1B}) \gamma(\vec{b} + \vec{s}_{2A} - \vec{s}_{2B}) \gamma(\vec{b} + \vec{s}_{3A} - \vec{s}_{3B}) \right| 0_A 0_B \rangle \quad (18a)$$

$$+ \frac{1}{6} AB(B-1)(B-2) \langle 0_A 0_B \left| \gamma(\vec{b} + \vec{s}_{1A} - \vec{s}_{1B}) \gamma(\vec{b} + \vec{s}_{1A} - \vec{s}_{2B}) \gamma(\vec{b} + \vec{s}_{1A} - \vec{s}_{3B}) \right| 0_A 0_B \rangle \quad (18b)$$

$$+ \frac{1}{6} A(A-1)(A-2)B \langle 0_A 0_B | \gamma(\vec{b} + \vec{s}_{1A} - \vec{s}_{1B}) \gamma(\vec{b} + \vec{s}_{2A} - \vec{s}_{1B}) \gamma(\vec{b} + \vec{s}_{3A} - \vec{s}_{1B}) | 0_A 0_B \rangle \quad (18c)$$

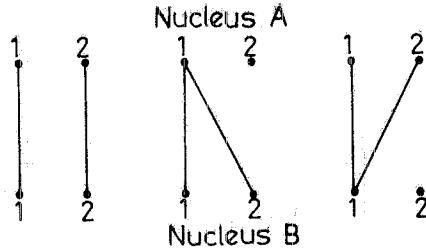
$$+ A(A-1)B(B-1) \langle 0_A 0_B | \gamma(\vec{b} + \vec{s}_{1A} - \vec{s}_{1B}) \gamma(\vec{b} + \vec{s}_{2A} - \vec{s}_{1B}) \gamma(\vec{b} + \vec{s}_{2A} - \vec{s}_{2B}) | 0_A 0_B \rangle \quad (18d)$$

$$+ \frac{1}{2} AB(B-1)(A-1)(B-2) \langle 0_A 0_B | \gamma(\vec{b} + \vec{s}_{1A} - \vec{s}_{1B}) \gamma(\vec{b} + \vec{s}_{1A} - \vec{s}_{2B}) \gamma(\vec{b} + \vec{s}_{2A} - \vec{s}_{3B}) | 0_A 0_B \rangle \quad (18e)$$

$$+ \frac{1}{2} A(A-1)B(A-2)(B-1) \langle 0_A 0_B | \gamma(\vec{b} + \vec{s}_{1A} - \vec{s}_{1B}) \gamma(\vec{b} + \vec{s}_{2A} - \vec{s}_{1B}) \gamma(\vec{b} + \vec{s}_{3A} - \vec{s}_{2B}) | 0_A 0_B \rangle \quad (18f)$$

where, for simplicity, we have assumed that the elementary profiles for the p-p and p-n interaction are identical. The consecutive terms in Eqs. (17) and (18) are visualized in Fig. 1.

DOUBLE SCATTERING



TRIPLE SCATTERING

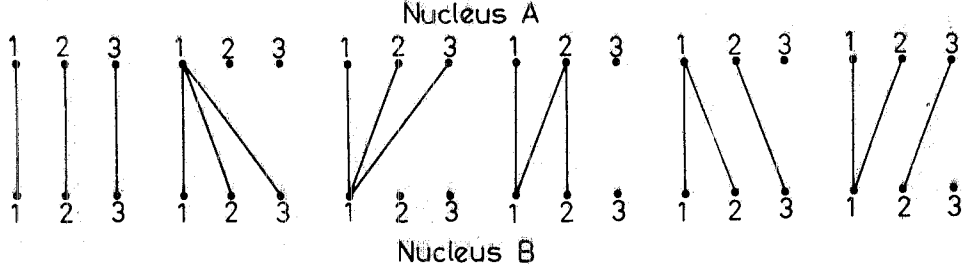


FIG. 1 - Diagrammatic description of the double- and triple-scattering processes.

For $n \geq 2$ one can distinguish between the terms with repetition of the nucleon coordinates (see Eqs. (17b, c), (18b-f)) and the terms without any repetition (Eq. (17a), (18a)). The number of the latter is $n! \binom{A}{n} \binom{B}{n}$; these terms can be calculated relatively easy. However, the repetition terms are much more difficult to treat. A large variety of such terms in scattering of two complex nuclei makes an evaluation of the ground state expectation value in Eq. (13) very laborious even for simple model wave functions.

Due to alternative signs in the series (14) and (15) different orders of scattering may interfere with each other in a destructive way. The most important result of this interference is the diffractive structure (maxima and minima) of the elastic differential cross-section. Of particular significance is also the effect of non-additivity in the total nucleus-nucleus cross-section:

$$\sigma_{AB} \ll AB \sigma_{NN} \quad (19)$$

The ground state expectation value in Eq. (13) may be evaluated using the independent-particle model:

$$\begin{aligned} \langle 0_A | \vec{r}_{1A}, \dots, \vec{r}_{AA} \rangle^2 &= \prod_{j=1}^A \varrho_A(r_{jA}) , \\ \langle 0_B | \vec{r}_{1B}, \dots, \vec{r}_{BB} \rangle^2 &= \prod_{k=1}^B \varrho_B(r_{kB}) , \end{aligned} \quad (20)$$

with the single-particle density in the form:

$$\varrho(r) = \pi^{-3/2} R^{-3} \exp\left(-\frac{r^2}{R^2}\right) . \quad (21)$$

As it is well known the use of Gaussian densities allows us to simply impose the condition of translational invariance⁽¹³⁾ on the nuclear densities (20). The c.m. constraint results in a simple multiplicative correction to the nucleus-nucleus scattering amplitude of Eq. (9)⁽⁸⁾. One has:

$$F_{G1}(q) = ik \exp\left(+\frac{q^2 R_A^2}{4A} + \frac{q^2 R_B^2}{4B}\right) \int_0^\infty db b J_0(qb) \left[\Gamma_0^{(1)}(b) + \Gamma_0^{(2)}(b) + \dots + \Gamma_0^{(AB)} \right] , \quad (22)$$

where the index $_0$ denotes the neglect of the centre-of-mass correlations. In order to obtain the nuclear profile which includes these correlations one should perform the Fourier-Bessel transform of Eq. (22):

$$\begin{aligned} \Gamma_{G1}(b) &= \int_0^\infty dq q \exp\left(+\frac{q^2 R_A^2}{4A} + \frac{q^2 R_B^2}{4B}\right) \cdot \\ &\cdot \int_0^\infty db' b' J_0(qb) J_0(qb') \Gamma_0(b') . \end{aligned} \quad (23)$$

In Fig. 2 we have compared various contributions to the ${}^4\text{He}-{}^4\text{He}$ elastic scattering cross-section in the Glauber model. The calculations were performed using the nuclear densities (21) and assuming the elementary profile function in the form:

$$\gamma(b) = \frac{\sigma(1 - i\alpha)}{4\pi a} \exp\left(-\frac{b^2}{2a}\right) , \quad (24)$$

which corresponds to a Gaussian q -dependence of the N-N scattering amplitude:

$$f(q) = \frac{ik\sigma(1 - i\alpha)}{4\pi} \exp\left(-\frac{1}{2} a q^2\right) . \quad (25)$$

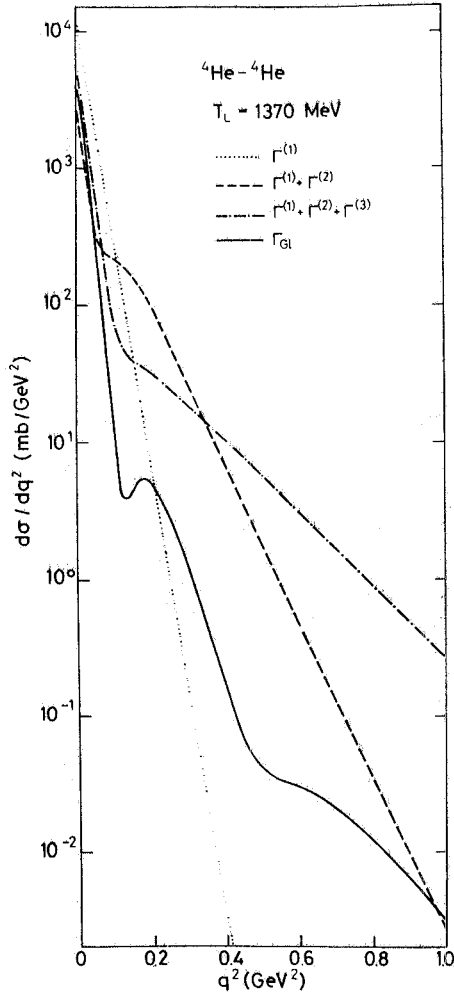


FIG. 2 - The angular distributions of the ${}^4\text{He}-{}^4\text{He}$ elastic scattering corresponding to the series of multiple scattering (14, 15) in the Glauber model. The nuclear Gaussian radii are $R_A = R_B = 1.37$ fm. The nucleon parameters at ~ 350 MeV/nucleon⁽¹⁴⁾ are $\sigma = 28$ mb, $\alpha = -0.45$, $a = 1.5$ GeV⁻².

The parameters σ (total nucleon-nucleon cross-section), a (Re/Im ratio of the forward amplitude) and α (slope) are, in general, energy dependent. The assumptions (20) and (24) allow to obtain analytical expressions for the nuclear profile and the scattering amplitude⁽⁸⁾.

Fig. 2 illustrates the mechanism of interference between various orders of scattering. The single scattering contribution largely overestimates the cross-section at small momentum transfers; this feature has been expressed by the inequality (19). The remedy is provided by a strong destructive interference of higher orders. Another result of the interference are the minima and secondary maxima of the angular distribution at large momentum transfers. It should be stressed that the convergence of the multiple scattering expansion based on Eq. (15) (we may call it the profile expansion) is rather slow. Very many terms have to be included in order to obtain the correct result.

3. - THE OPTICAL MODEL OF MULTIPLE SCATTERING.

The eikonal approximation implied in the Glauber model may be surpassed by introducing the concept of the optical potential of multiple scattering⁽¹⁴⁾. This potential leads to another multiple-scattering expansion which, as we shall see, converges much faster than the profile expansion of Eq. (15).

The optical potential is constructed by exploiting the well-known fact that in the eikonal limit of quantum scattering the inverse scattering problem can be easily solved⁽⁶⁾. Thus if at the eikonal limit $G \rightarrow G_{\text{eik}}$ (G and G_{eik} being the exact and eikonal free Green's functions, respectively) one has for the scattering matrix element on the energy-shell:

$$T \rightarrow T_{\text{eik}}(q) = -2\pi i v \int_0^{\infty} dq q J_0(qb) \Gamma_{\text{eik}}(b), \quad (26)$$

then the optical potential:

$$V = T_{\text{eik}}(1 + G_{\text{eik}} T_{\text{eik}})^{-1}, \quad (27)$$

can be reduced, under an assumption of a spherically symmetric interaction, to the following formula:

$$V(r) = -\frac{2iv}{\pi} \int_0^{\infty} dz \frac{d}{dr^2} \ln \left[1 - \Gamma_{\text{eik}}(\sqrt{r^2 + z^2}) \right]. \quad (28)$$

The essential point is that the linearization of the propagator implied in the eikonal limit⁽¹⁶⁾ does not affect the interaction. Hence the optical potential (27, 28), although obtained with the aid of the approximate amplitude and propagator, does represent the true interaction. The use of this potential in the Schrödinger equation, being solved without any approximation, will provide the correct description of the scattering.

Now, the eikonal profile Γ_{eik} of Eq. (26) can be identified with the nuclear profile Γ_{G1} of the Glauber model. This is justified since the Glauber model may be considered as a transposition of the rigorous Watson theory of multiple collision⁽¹⁵⁾ to the eikonal mechanics^(16, 17) under the usual assumptions of closure and impulse approximations. Inserting potential (28) with the assumption $\Gamma_{\text{eik}} = \Gamma_{\text{G1}}$ into the wave equation one obtains for the scattering matrix:

$$T = V(1 - \mathbf{GV})^{-1} = T_{\text{G1}} + T(\mathbf{G} - \mathbf{G}_{\text{eik}})T_{\text{G1}} = T_{\text{G1}} + T_{\text{G1}}(\mathbf{G} - \mathbf{G}_{\text{eik}})T_{\text{G1}} + \dots \quad (29)$$

The use of the optical potential can thus be regarded as an implicit summation of the eikonal expansion⁽¹⁸⁾ is given by Glauber's scattering amplitude T_{G1} . Indeed this eikonal expansion represents the main contents of Watson's multiple scattering series. It can be shown that the remaining corrections, coming from the nuclear Hamiltonian and from the transfor

mation between the nucleon-nucleon and nucleus-nucleus c. m. systems⁽¹⁹⁾, tend to cancel each other⁽¹⁷⁾.

Using Eq. (15) the logarithm in Eq. (28) can be expanded:

$$\begin{aligned} -\ln(1 - \Gamma_{G1}) &= \Gamma_{G1} + \frac{1}{2} \Gamma_{G1}^2 + \frac{1}{3} \Gamma_{G1}^3 + \dots = \\ &= \Gamma^{(1)} + \left[\Gamma^{(2)} + \frac{1}{2} (\Gamma^{(1)})^2 \right] + \left[\Gamma^{(3)} + \Gamma^{(1)} \Gamma^{(2)} + \frac{1}{3} (\Gamma^{(1)})^3 \right] + \dots \end{aligned} \quad (30)$$

From here a multiple-scattering expansion of the optical potential follows⁽²⁰⁾:

$$V(r) = V^{(1)} + V^{(2)} + V^{(3)} + \dots, \quad (31)$$

where

$$V^{(1)}(r) = \frac{2iv}{\pi} \int_0^\infty dz \Gamma^{(1)}(\sqrt{r^2 + z^2}), \quad (32a)$$

$$V^{(2)}(r) = \frac{2iv}{\pi} \int_0^\infty dz \left[\Gamma^{(2)} + \Gamma^{(1)} \Gamma^{(1)} \right], \quad (32b)$$

$$V^{(3)}(r) = \frac{2iv}{\pi} \int_0^\infty dz \left[\Gamma^{(3)} + \Gamma^{(1)} \Gamma^{(2)} + \Gamma^{(1)} \Gamma^{(2)} + (\Gamma^{(1)})^2 \Gamma^{(1)} \right], \quad (32c)$$

etc.

with

$$\Gamma^{(n)} \equiv \frac{d}{dr^2} \Gamma^{(n)}(\sqrt{r^2 + z^2}).$$

Let us discuss in details the first order approximation to the potential. Since

$$\Gamma^{(1)}(\sqrt{r^2 + z^2}) = \frac{1}{ik} \int_0^\infty dq q J_0(q\sqrt{r^2 + z^2}) F^{(1)}(q), \quad (33)$$

$F^{(1)}(q)$ being the single scattering contribution to the scattering amplitude, the use of the identity

$$j_0(qr) = -\frac{2}{q} \frac{d}{dr^2} \int_0^\infty dz J_0(q\sqrt{r^2 + z^2}), \quad (34)$$

allows to transform Eq. (32a) into the form:

$$V^{(1)}(r) = \frac{1}{2\pi^2} \int_0^\infty dq q^2 j_0(qr) \left[-\frac{2\pi v}{k} F^{(1)}(q) \right]. \quad (35)$$

Hence the Fourier transform of the spherically symmetric potential $V^{(1)}(r)$ can be written as

$$V^{(1)}(q) = \left\langle 0_A 0_B \left| \sum_{j=1}^A \sum_{k=1}^B t_{jk}(q) e^{i\vec{q} \cdot \vec{r}_{jA}} e^{-i\vec{q} \cdot \vec{r}_{kB}} \right| 0_A 0_B \right\rangle, \quad (36)$$

that is exactly the well-known expression for the first order approximation to the optical potential as given in Watson's theory of multiple collision⁽¹⁵⁾.

Obviously, the Watson potential of Eq. (36) gives more than a single scattering amplitude. This can be seen by considering the Born expansion of the scattering matrix :

$$T = V^{(1)} + V^{(1)}GT = V^{(1)} + V^{(1)}GV^{(1)} + V^{(1)}GV^{(1)}GV^{(1)} + \dots \quad (37)$$

Thus, in contrast to the profile expansion of Eq. (15), the potential expansion (Eq. (31)) gives, already in its first term, rise to multiple-scattering effects. However, it should be pointed out (see also Chapter 4) that the Watson potential corresponds to a scattering matrix which neglects the quasi-elastic shadowing^(21, 22), i. e. the virtual excitations of colliding nuclei in intermediate states. Therefore, one may refer to the first-order potential as to the static optical potential. Contrary the multiple-scattering potential of Eq. (28) is a dynamic one since it admits the possibility of intermediate excitations.

Assuming the scattering matrices t for the p-p, p-n and n-n systems as identical Eq. (36) may be written in the form :

$$V^{(1)}(q) = - \frac{2\pi v}{k} AB f(q) \Phi_A(q) \Phi_B(q) \quad (38)$$

where

$$\Phi_A = \frac{1}{A} \langle 0_A | \sum_{j=1}^A e^{i\vec{q} \cdot \vec{r}_{jA}} | 0_A \rangle, \quad \Phi_B = \frac{1}{B} \langle 0_B | \sum_{k=1}^B e^{-i\vec{q} \cdot \vec{r}_{kB}} | 0_B \rangle \quad (39)$$

are the elastic form factors of the two nuclei and $f(q)$ is the nucleon-nucleon elastic scattering amplitude. This leads to a simple double-folding formula for the optical potential :

$$V^{(1)}(r) = AB \int d^3 r_A d^3 r_B \varrho_A(r_A) t(\vec{r} + \vec{r}_A - \vec{r}_B) \varrho_B(r_B) \quad (40)$$

where ϱ_A, ϱ_B are the nuclear densities, i. e. the Fourier transforms of the form factors Φ_A, Φ_B .

A frequent approximation of Eq. (38) is to put :

$$f(q) \approx f(0) = \frac{k\sigma(i + \alpha)}{4\pi} \quad (41)$$

This is justified since the nuclear form factors fall down with the momentum transfer more rapidly than the amplitude of elementary scattering. This approximation corresponds to a zero-range t -matrix and gives the optical potential as the convolution of the nuclear densities :

$$V^{(1)}(r) = - \frac{v\sigma(i + \alpha)}{2} AB \int d^3 r' \varrho_A(\vec{r} - \vec{r}') \varrho_B(\vec{r}') \quad (42)$$

It is expected that the potential expansion of Eq. (31) will be, due to effects of multiple scattering arising from higher Born terms, sufficiently fast convergent. This would allow to avoid enormous complications connected with the calculation of the Glauber profile for complex nuclei. Instead of the complete profile, only a few first terms in the profile expansion (15) that appear in Eq. (32) would need to be calculated. This expectation is basically confirmed by the comparisons shown in Figs. 3 and 4.

In general, the rate of convergence of the series (31) to Eq. (28) depends on the momentum transfer and the complexity of colliding nuclei ; larger the momentum transfer and heavier nuclei greater the number of terms have to be included. From the comparison of Fig. 2 and Fig. 3 the superiority of the potential expansion (31) over the profile expansion (15) is evident. For the ${}^4\text{He}$ - ${}^4\text{He}$ system up to $q = 1$ GeV/c the potential expansion is practically saturated in the third order while in the profile expansion of the scattering amplitude one would need at least six orders of scattering. For the ${}^4\text{He}$ - ${}^{12}\text{C}$ system in order to achieve the convergence shown in Fig. 4 the profile expansion would require more than ten orders of scattering⁽²³⁾.

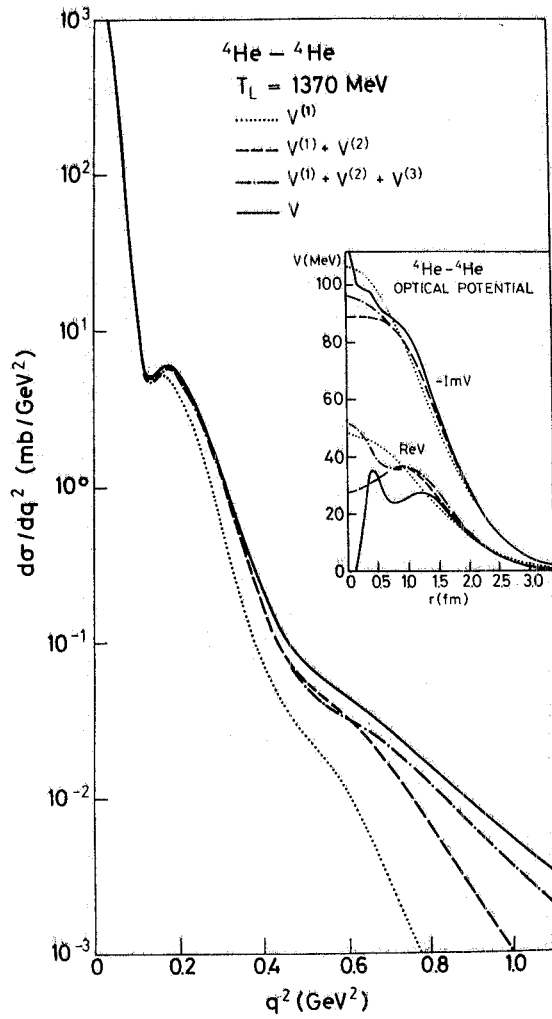


FIG. 3 - The angular distributions of the ${}^4\text{He}-{}^4\text{He}$ elastic scattering corresponding to various approximations (see Eqs. (32)) to the potential of multiple scattering, shown in the inset. Same parameters as in Fig. 2.

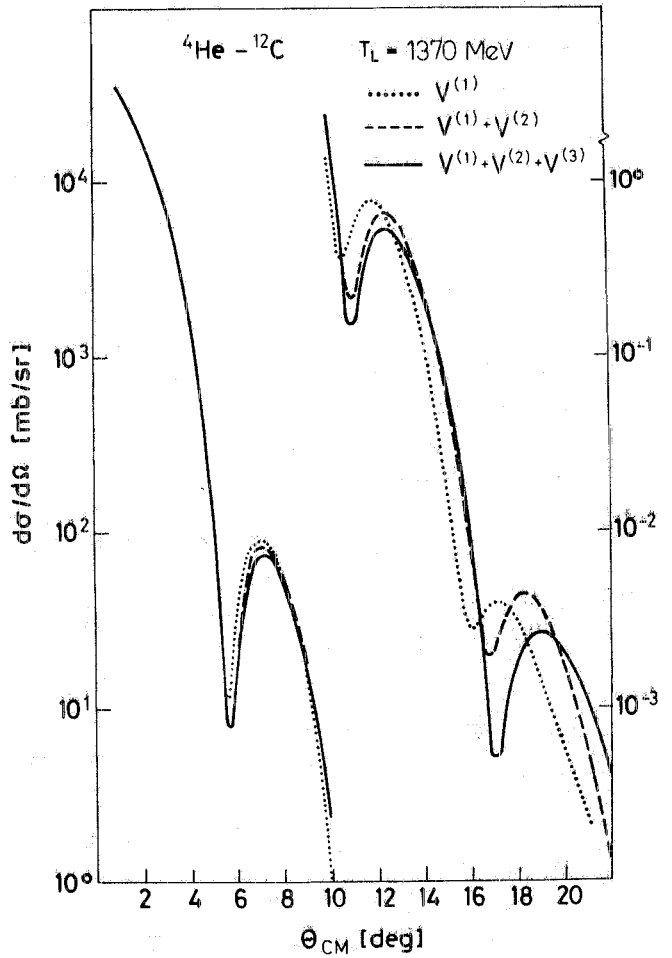


FIG. 4 - The angular distributions of the ${}^4\text{He}-{}^{12}\text{C}$ elastic scattering corresponding to various approximations (see Eqs. (32)) to the potential of multiple scattering. The Coulomb interaction included. The parameters $R_4 = 1.37$ fm, $R_{12} = 1.93$ fm, $\sigma = 28$ mb, $\alpha = 0.3$, $a = 1.5$ GeV $^{-2}$.

The potential and profile expansion differ not only by the rate of convergences. The use of the optical potential in the wave equation allows to account for the effects of non-eikonal propagation which are obviously absent when the scattering amplitude is calculated as the Fourier-Bessel transform of the eikonal Glauber profile.

The non-eikonal effects are particularly important at diffractive minima and at large momentum transfers. The results obtained by exactly solving the Schrödinger equation turned out to be very sensitive to the sign of the real part of the optical potential. Specifically, the repulsive interaction (corresponding to negative values of the elementary parameter α , see Eq. (42)) fills the minima up while the attractive interaction ($\alpha > 0$) makes them deeper - see Fig. 5. In contrast, the results based upon the eikonal Glauber model are independent of the sign of $\alpha^{(x)}$.

(x) - When the Coulomb interaction is included also the Glauber results depend on sign of $\alpha^{(11)}$. However, for light nuclei, where the Coulomb interaction is of a minor importance, the sensitivity of nuclear scattering to the repulsive or attractive character of the elementary force originates mainly from the non-eikonal propagation.

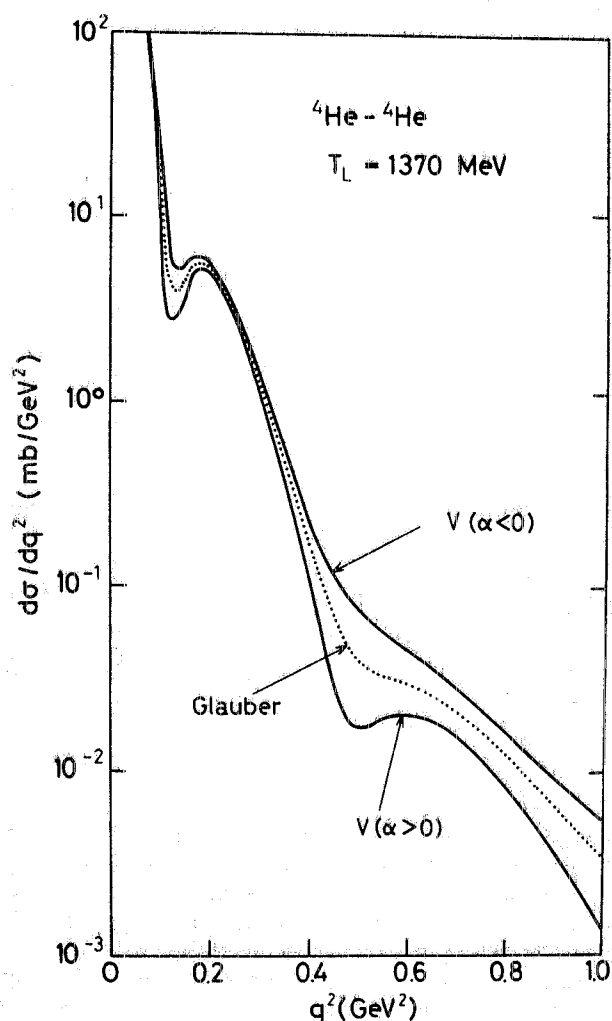


FIG. 5 - The differential cross-section of ${}^4\text{He}-{}^4\text{He}$ elastic scattering in the Glauber model (dotted curve) and in the optical model with the potential of multiple scattering (28) (solid curves). No Coulomb interaction. Parameters: $R_A = R_B = 1.37$ fm, $\sigma = 28$ mb, $\alpha = \pm 0.45$, $a = 1.5$ GeV^{-2} . The Glauber curve is insensitive to the sign of α .

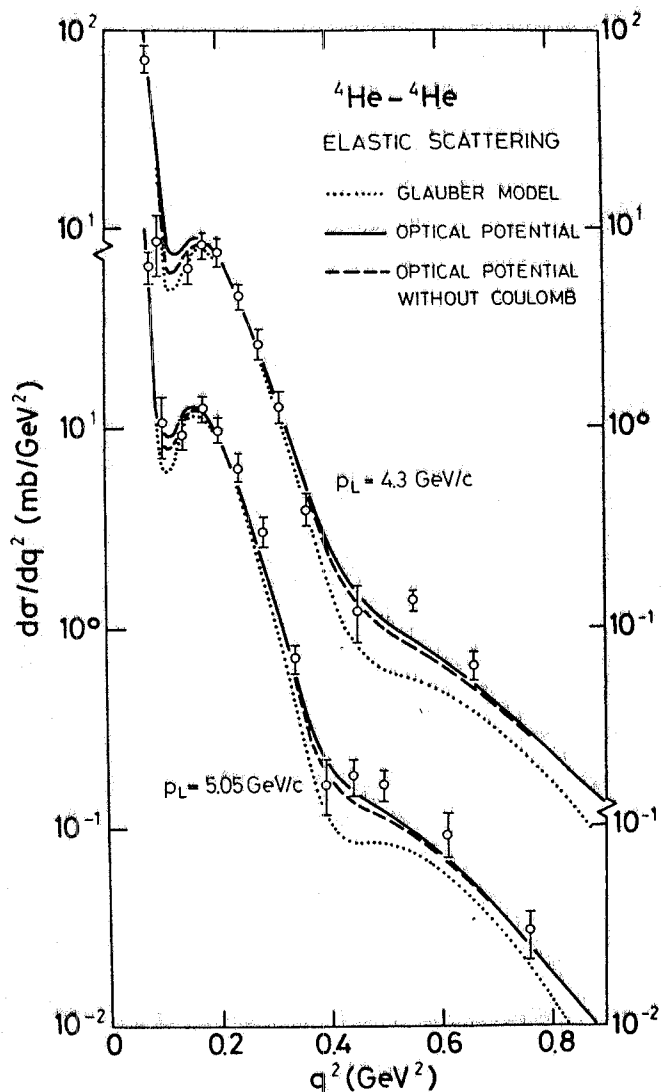


FIG. 6 - The differential cross-section of ${}^4\text{He}-{}^4\text{He}$ elastic scattering⁽²⁰⁾. Dotted curves correspond to the Glauber model, dashed and solid (including the Coulomb interaction) ones to the optical model of multiple scattering. Experimental data are taken from ref. (24). The nuclear parameters are $R_A = R_B = 1.37$ fm. The nucleon parameters are taken as average values quoted in the literature^(26, 27): $\sigma = 32.25$ mb, $\alpha = -0.43$, $a = 1.7$ GeV^{-2} at $p_L = 4.3$ GeV/c , and $\sigma = 39.3$ mb, $\alpha = -0.4$, $a = 3.4$ GeV^{-2} at $p_L = 5.05$ GeV/c .

In Fig. 6 the angular distributions for the ${}^4\text{He}-{}^4\text{He}$ elastic scattering obtained in the optical model (solid and dashed curves) and the Glauber model predictions (dotted curve) are compared with the experimental data⁽²⁴⁾. It is evident that agreement with the experiment is considerably improved when accounting for the non-eikonal propagation with the aid of the optical potential. The role of the Coulomb potential in filling the minima up is significant (though not as great as stated in ref. (25)) and increases with increasing nuclear masses.

The potential expansion (31) may be used to reorder the expansion (15) of the Glauber profile. This has been first done by Franco and Varma⁽²⁸⁾. In fact, applying the eikonal approximation

(5, 6) to the optical potential (31) the nuclear profile may be written as :

$$\Gamma_{\text{Gl}}^{(b)} = 1 - e^{i[\chi^{(1)}(b) + \chi^{(2)}(b) + \chi^{(3)}(b) + \dots]} \quad (43)$$

where

$$\chi^{(n)} = -\frac{1}{v} \int_{-\infty}^{+\infty} dz V^{(n)}(\sqrt{b^2 + z^2}) \quad (44)$$

Now using the identity :

$$\chi_{\text{Gl}} = \chi^{(1)} + \chi^{(2)} + \chi^{(3)} + \dots = -i \ln(1 - \Gamma_{\text{Gl}}) \quad (45)$$

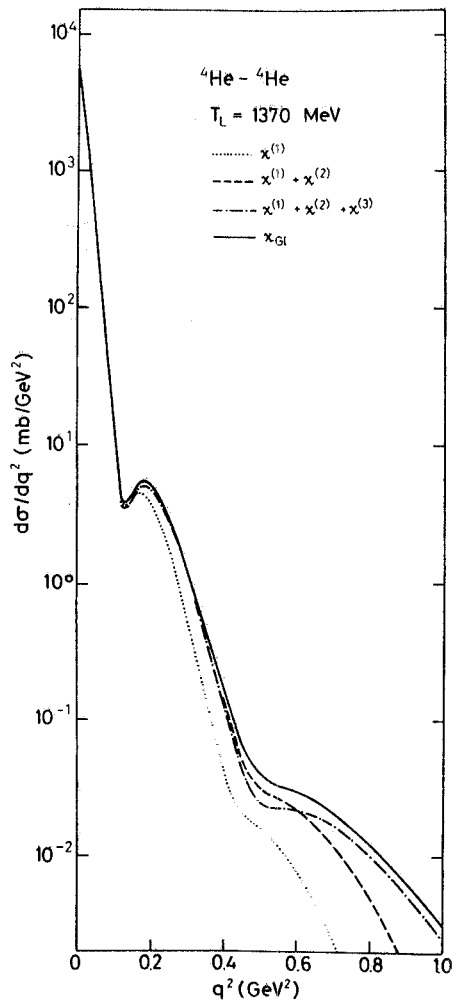
one obtains from (30)

$$\chi^{(1)}(b) = i \Gamma^{(1)}(b) \quad (46a)$$

$$\chi^{(2)}(b) = i \left[\Gamma^{(2)}(b) + \frac{1}{2} (\Gamma^{(1)}(b))^2 \right] \quad (46b)$$

$$\chi^{(3)}(b) = i \left[\Gamma^{(3)}(b) + \Gamma^{(1)}(b) \Gamma^{(2)}(b) + \frac{1}{3} (\Gamma^{(1)}(b))^3 \right] \quad (46c)$$

etc.

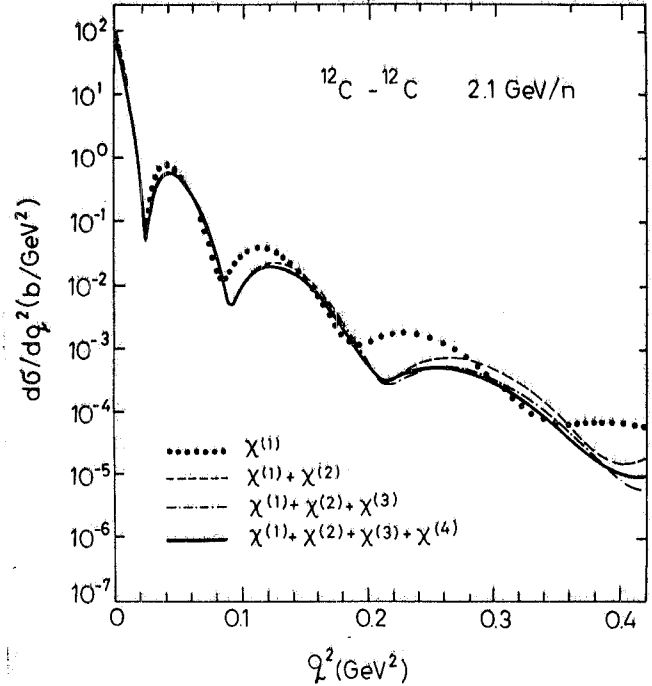


The expansion (43) can of course be formally obtained from (45) without any reference to the optical potential (28). However, the close relation between the phase-shift and the potential underlies the expectation that the phase-shift expansion (43) will be much faster converging than the profile expansion (15). In fact, the eikonal phase-shift, like the potentials, give rise to multiple scattering effects, generated by higher order terms in the Born expansion of the eikonal scattering matrix. The convergence of the phase-shift and potential expansions should therefore be quite similar. The comparison of Figs. 3 and 7 confirms this prediction.

FIG. 7 - The angular distributions of the ${}^4\text{He}-{}^4\text{He}$ elastic scattering corresponding to the phase-shift expansion (Eq. (43)) in the Glauber model. Same parameters as in Fig. 2.

The phase-shift expansion can be considered as the eikonal counterpart of the potential expansion of the scattering amplitude. At sufficiently high energies one may rely on the eikonal approximation and use only the phase-shift expansion (43) avoiding this way serious complications connected with exactly solving the Schrödinger equation. Another example of the phase-shift expansion is given in Fig. 8^{(29)(x)}.

FIG. 8 - The angular distributions of the $^{12}\text{C}-^{12}\text{C}$ elastic scattering at 2.1 GeV/n corresponding to the phase-shift expansion (Eq. (43)) in the Glauber model⁽²⁹⁾. The nuclear Gaussian radii are $R_A = R_B = 1.97$ fm. The nucleon parameters are $\sigma = 42.7$ mb, $\alpha = -0.28$, $a = 6.2$ GeV⁻².



4. - QUASI-ELASTIC SHADOWING IN NUCLEUS-NUCLEUS COLLISIONS.

As the number of nucleons in the colliding nuclei increases the evaluation of the full multiple scattering series (15) becomes more intractable. Complete calculations have been carried out only for light systems like $^4\text{He}-^4\text{He}$ and $^2\text{H}-^{16}\text{O}$, using Gaussians wave functions⁽⁸⁾. In the preceding section we have discussed how the use of the potential and phase-shift expansions can allow to overcome the calculational difficulties. However, this appears to be a practical way but for light and medium nuclei. Instead, for heavy nuclei the problem is not solved, as had firstly been indicated by Franco and Varma^(23, 29). For large A and B, contrary to prevalent belief^(o), the higher order terms begin to dominate (e. g. $|\chi^{(1)}| < |\chi^{(2)}| < |\chi^{(3)}| < \dots$), rendering the above expansions useless.

In this chapter we present a non-perturbative approach to multiple scattering in the nucleus-nucleus collisions. Some approximations to the Glauber formula (13) are obtained by partially neglecting the intermediate excitations of the colliding nuclei. This approach originates as a result of reconsidering the assumption of closure which underlies the multiple scattering model. Closure assumes the energetic degeneracy of the nuclear eigenstates. However, it does include a possibility of excitations and de-excitations (linked each to other in such a way that the final result would be elastic scattering) of the two nuclei during collision. The effect of virtual nuclear excitations will be referred to as the quasi-elastic shadowing^(21, 30).

The closure approximation gives rise to ground state expectation values of multibody operators which result from summation over all the possible intermediate excitations (see Eq. (1)).

(x) - There are different ways of presenting the phase-shift expansion related to the manner of introducing the centre-of-mass constraint⁽²⁹⁾. We assume here^(21, 30) that the nuclear ground states $|0_A\rangle$, $|0_B\rangle$ are intrinsic states hence all the expectation values as profiles (see Eq. (23)), potentials and phase-shifts inherently contain the effect of translational invariance.

(o) - In particular the first order approximation, referred to as the optical limit⁽⁸⁾, turns out to be inaccurate. This approximation has been frequently employed to study elastic scattering⁽³¹⁻³³⁾ and fragmentation processes⁽³⁴⁾.

It is instructive to show these sums explicitly. As an example let us write two of the third-order contributions (18) to the profile function (13) as follows :

$$\begin{aligned} & \langle 0_A 0_B | \gamma(\vec{b} + \vec{s}_{1A} - \vec{s}_{1B}) \gamma(\vec{b} + \vec{s}_{2A} - \vec{s}_{1B}) \gamma(\vec{b} + \vec{s}_{3A} - \vec{s}_{1B}) | 0_A 0_B \rangle = \\ & = \sum_{|n_A\rangle |n'_A\rangle |n_B\rangle |n'_B\rangle} \langle 0_A 0_B | \gamma(\vec{b} + \vec{s}_{1A} - \vec{s}_{1B}) | n_A n_B \rangle \cdot \end{aligned} \quad (47c)$$

$$\cdot \langle n_A n_B | \gamma(\vec{b} + \vec{s}_{2A} - \vec{s}_{1B}) | n'_A n'_B \rangle \langle n'_A n'_B | \gamma(\vec{b} + \vec{s}_{3A} - \vec{s}_{1B}) | 0_A 0_B \rangle ,$$

$$\begin{aligned} & \langle 0_A 0_B | \gamma(\vec{b} + \vec{s}_{1A} - \vec{s}_{1B}) \gamma(\vec{b} + \vec{s}_{2A} - \vec{s}_{1B}) \gamma(\vec{b} + \vec{s}_{2A} - \vec{s}_{2B}) | 0_A 0_B \rangle = \\ & = \sum_{|n_A\rangle |n'_A\rangle |n_B\rangle |n'_B\rangle} \langle 0_A 0_B | \gamma(\vec{b} + \vec{s}_{1A} - \vec{s}_{1B}) | n_A n_B \rangle \cdot \end{aligned} \quad (47d)$$

$$\cdot \langle n_A n_B | \gamma(\vec{b} + \vec{s}_{2A} - \vec{s}_{1B}) | n'_A n'_B \rangle \langle n'_A n'_B | \gamma(\vec{b} + \vec{s}_{2A} - \vec{s}_{2B}) | 0_A 0_B \rangle ,$$

where the summations extend over the complete set of states for the two nuclei.

The complete neglecting of quasi-elastic shadowing (NS) is equivalent to putting $|n_A\rangle = |n'_A\rangle = |0_A\rangle$ and $|n_B\rangle = |n'_B\rangle = |0_B\rangle$ in Eqs. (47). Generally such a procedure would lead to the following expression for the nucleus-nucleus profile (13) :

$$\begin{aligned} \Gamma^{NS}(b) &= 1 - \prod_{j=1}^A \prod_{k=1}^B \left[1 - \langle 0_A 0_B | \gamma_{jk}(\vec{b} + \vec{s}_{jA} - \vec{s}_{kB}) | 0_A 0_B \rangle \right] = \\ &= 1 - \left[1 - \langle 0_A 0_B | \gamma(\vec{b} + \vec{s}_{1A} - \vec{s}_{1B}) | 0_A 0_B \rangle \right]^{AB} . \end{aligned} \quad (48)$$

The expression which is formally identical to Eq. (48) has been obtained by Czyz and Maximon⁽⁸⁾ in a consideration of so-called optical limit of the multiple scattering. In the present approach Eq. (48) is obtained by only ignoring the quasi-elastic shadowing, without any assumptions about the nuclear ground-state wave functions. Thus the optical limit acquires a new physical meaning as being essentially equivalent to neglecting intermediate excitations of the nuclei during collision.

Since the nuclear ground states $|0_A\rangle$, $|0_B\rangle$ are intrinsic states the new optical limit (Eq. (48)) inherently includes the effect of translational invariance⁽¹³⁾ which is of crucial importance for light nuclei. This should be contrasted with the usual approach to the optical limit where the correction arising from the centre-of-mass constraint is introduced inconsistently, leading to a divergence at large momentum transfer^(8, 35). In order to better explain this difference let us rewrite the basic component of Eq. (48) as follows :

$$\langle 0_A 0_B | \gamma(\vec{b} + \vec{s}_{1A} - \vec{s}_{1B}) | 0_A 0_B \rangle = \frac{1}{2\pi i k} \int d^2q e^{-i\vec{q} \cdot \vec{b}} f(q) \Phi_A(q) \Phi_B(q) , \quad (49)$$

where Φ_A , Φ_B are the elastic form factors (39) of the two nuclei. In our approach the centre-of-mass correction enters through the form factors Φ_A and Φ_B while in the standard treatment Φ_A and Φ_B are unaffected by the c. m. constraint and an overall correction factor is being applied to the nucleus-nucleus scattering amplitude. This correction may, however, turn out to be an una-

dequate one if one approximates the multiple-scattering series as it is the case in the standard derivation of the optical limit.

The results for the ${}^4\text{He}-{}^4\text{He}$ elastic scattering presented in Fig. 9⁽³⁰⁾ clearly show the superiority of the new optical limit over the old one. In the present approach the agreement of Eq.

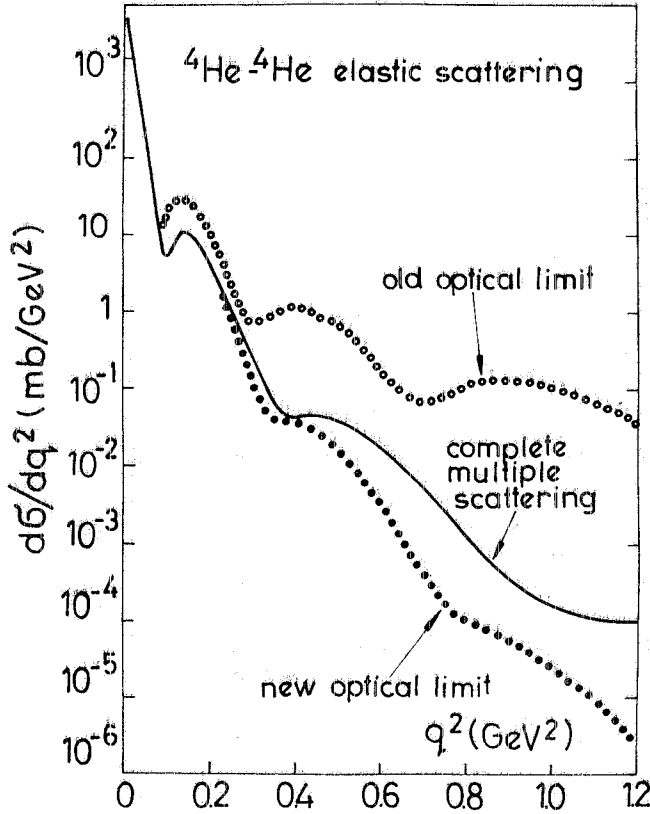


FIG. 9 - The differential cross-section of ${}^4\text{He}-{}^4\text{He}$ elastic scattering in various versions of the Glauber model. The new (Eq. (48)) and old⁽⁸⁾ optical limit are compared with the complete multiple scattering calculation (Eq. (13)). The parameters are appropriate for several GeV incident alphas: $\sigma = 41$ mb, $\alpha = -0.33$, $a = 10$ GeV⁻². $R_A = R_B = 1.37$ fm.

(48) with the complete multiple scattering is being largely extended. The effect of quasi-elastic shadowing shows up only at large momentum transfers. The size of the shadowing might be a measure of appropriateness of nucleus-nucleus scattering as a tool for obtaining information on nuclear structure which cannot be available from electron scattering⁽²¹⁾, the latter measuring only the elastic form factors Φ_A, Φ_B .

For large A and B Eq. (48) can be exponentiated:

$$\Gamma^{\text{NS}(b)} = 1 - \exp \left[-AB \langle 0_A 0_B \cdot \right. \quad (50)$$

$$\left. \cdot \left[\gamma(\vec{b} + \vec{s}_{1A} - \vec{s}_{1B}) \right] \right],$$

which exactly coincides with the first order approximation in the phase-shift expansion (43). It should also be stressed that the optical potential (28) corresponding to this approximation of the nuclear profile coincides with the first order term in the potential expansion. The Watson optical potential (36) describes thus a static scattering process in which both the projectile and the target behave like rigid nuclei which cannot be excited.

It is reasonable to expect that an improvement to Eq. (48) could be obtained by allowing for virtual excitations in one of the colliding nuclei, say in the target B. If we still ignore the quasi-elastic shadowing in the projectile A (i. e. $|n_A\rangle = |n'_A\rangle = \dots = |0_A\rangle$) we obtain for the profile function:

$$\Gamma^{\text{RP}(b)} = 1 - \langle 0_B \left| \prod_{k=1}^B \left\{ \prod_{j=1}^A \left[1 - \langle 0_A \left| \gamma_{jk}(\vec{b} + \vec{s}_{jA} - \vec{s}_{kB}) \right| 0_A \rangle \right] \right\} \right| 0_B \rangle. \quad (51)$$

This approximation will be called the "rigid projectile" (RP). The analogous approximation for the target nucleus will be denoted RT.

Another improvement would be expected from allowing for at least a partial shadowing in the projectile A, having still the complete shadowing in the target B. The formula⁽³⁶⁾:

$$\Gamma^{\text{QSP}(b)} = 1 - \langle 0_B \left| \prod_{k=1}^B \left\{ \langle 0_A \left| \prod_{j=1}^A \left[1 - \gamma_{jk}(\vec{b} + \vec{s}_{jA} - \vec{s}_{kB}) \right] \right| 0_A \rangle \right\} \right| 0_B \rangle, \quad (52)$$

may be referred to as the "quasi-soft projectile" (QSP). It corresponds to putting $|n'_A\rangle = |0_A\rangle$, but $|n_A\rangle \neq |0_A\rangle$ in the case of Eq. (47d), and $|n_A\rangle \neq |n'_A\rangle \neq |0_A\rangle$ in the instance of Eq. (47c). Here the target nucleons can induce intermediate excitations in the projectile nucleus although each of them begins and finishes to collide with the projectile in its ground state. Various possibilities of virtual nuclear excitations for double and triple scattering are depicted in Fig. 10.

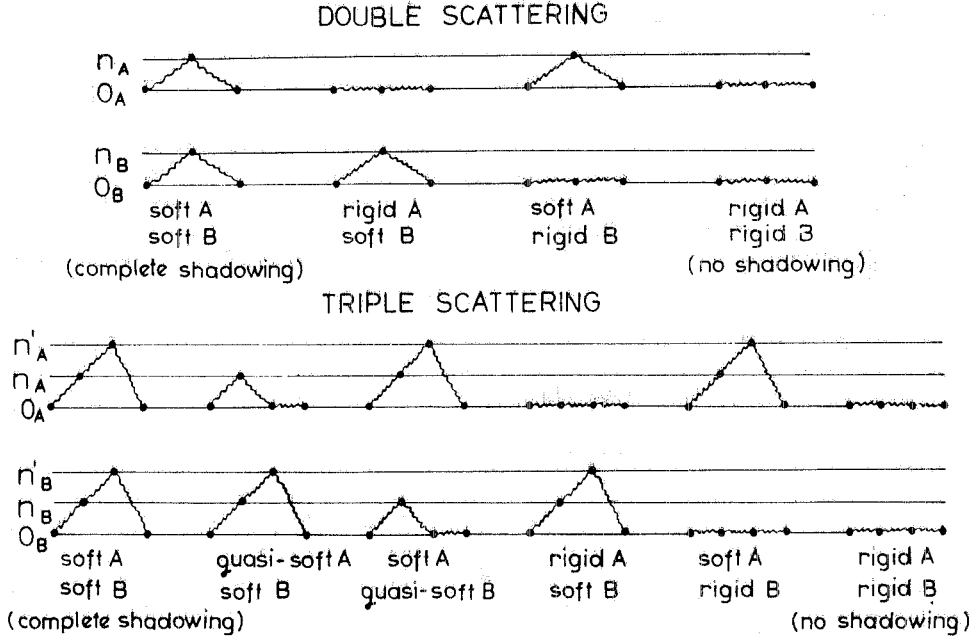


FIG. 10 - Diagrammatic description of virtual nuclear excitations for double- and triple-scattering.

It is instructive to write Eq. (52) as follows :

$$\Gamma^{\text{QSP}}(b) = 1 - \langle 0_B | \prod_{k=1}^B \left[1 - \Gamma_{AN}(\vec{b} - \vec{s}_{kB}) \right] | 0_B \rangle . \quad (53)$$

The QSP approximation has thus the form of the profile for nucleon-target nucleus scattering with the nucleon-projectile nucleus profile Γ_{AN} to replace the nucleon-nucleon profile γ_{NN} .

Similarly Eq. (51) can be rewritten as :

$$\Gamma^{\text{RP}}(b) = 1 - \langle 0_B | \prod_{k=1}^B \left[1 - \frac{1}{A} \Gamma_{AN}^{(1)}(\vec{b} - \vec{s}_{kB}) \right]^A | 0_B \rangle , \quad (54)$$

$\Gamma_{AN}^{(1)}$ being the single-scattering contribution to the profile Γ_{AN} . The RP approximation arises thus from Eq. (53) by applying the optical limit for the projectile nucleus.

Eq. (53) has been used in Refs. (37, 38) where it is called the "rigid projectile approximation". As it follows from our discussion this name would be more justified for Eqs. (51) and (54) because the formula (53) does admit the possibility of some virtual excitations of the projectile nucleus.

Both the approximations (51) and (52) are appealing because of a relative ease to evaluate them. The calculations are similar to those for proton-nucleus scattering except that the elementary profile is now composed of many terms. In Figs. 11 and 12 the quasi-soft and rigid projectile approximations for the ${}^4\text{He}$ - ${}^4\text{He}$ systems are compared to the no-shadowing formula (48) and the complete multiple-scattering calculation. This is done both for the Glauber scattering amplitude (Eq. (9)) and for the scattering amplitude resulting from the optical potential of multi-

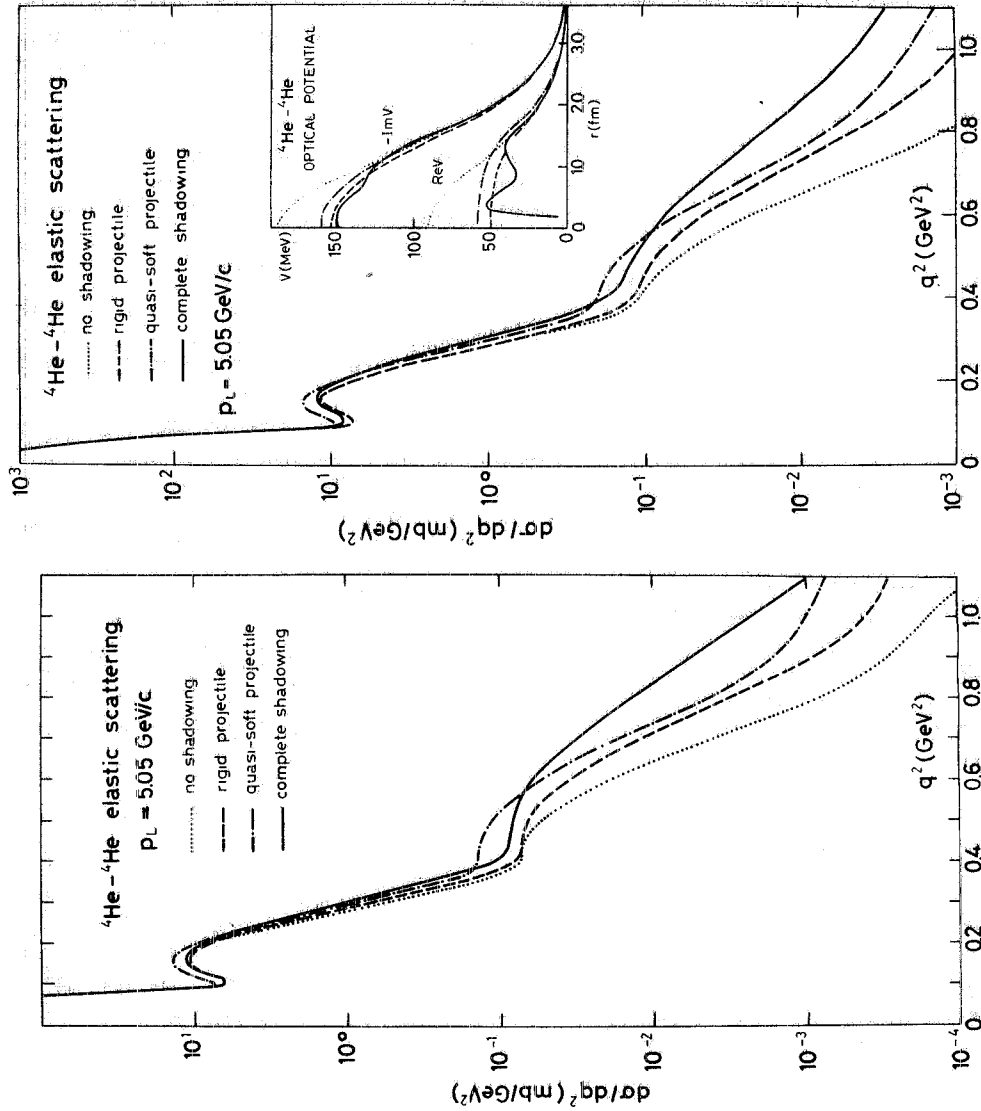


FIG. 11 - The differential cross-section of ${}^4\text{He}-{}^4\text{He}$ elastic scattering in the Glauber model, corresponding to various approximations to the nuclear profile. The no-shadowing (Eq. (48)), rigid projectile (Eq. (51)) and quasi-soft projectile (Eq. (52)) approximations are compared with the complete multiple-scattering calculations (Eq. (13)), the respective optical potentials being shown in the inset. Same parameters as in Fig. 11.

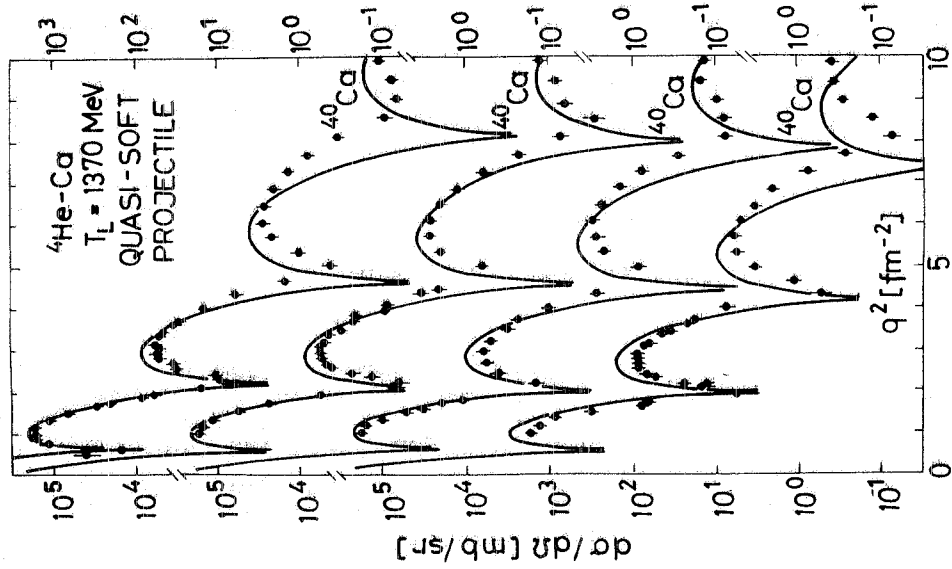


FIG. 13 - The differential cross-section for ${}^4\text{He}$ elastic scattering from several calcium isotopes. The quasi-soft projectile approximation to the Glauber model was used (38). The matter densities of the Ca isotopes were parametrized using a 3-parameter Fermi type distribution. The nucleon parameters are (39): $\sigma_{pp} = 24 \text{ mb}$, $\sigma_{pn} = 33 \text{ mb}$, $\alpha_{pp} = 0.65$, $\alpha_{pn} = 0.05$, $a_{pp} = 0.02 \text{ fm}^2$, $a_{pn} = 0.072 \text{ fm}^2$. The experimental data are from ref. (37).

FIG. 12 - The differential cross-section of ${}^4\text{He}-{}^4\text{He}$ elastic scattering in the optical model of multiple scattering corresponding to various approximations to the nuclear profile. The no-shadowing (Eq. (48)), rigid projectile (Eq. (51)) and quasi-soft projectile (Eq. (52)) approximations are compared with the complete multiple-scattering calculations (Eq. (13)), the respective optical potentials being shown in the inset. Same parameters as in Fig. 11.

ple scattering (Eq. (28)). It can be seen that by allowing for the quasi-elastic shadowing in one of the colliding nuclei the agreement with the complete calculation is considerably improved, particularly at large momentum transfer and at small distances. The difference between the approximations of quasi-soft and rigid projectile is, in general, small and it is hard to conclude which of the two is better.

In Fig. 13 the quasi-soft projectile approximation is confronted with the experimental results for the ${}^4\text{He}$ elastic scattering from various calcium isotopes. The eikonal Glauber model of multiple scattering with the Coulomb interaction included was used⁽³⁸⁾. The theoretical calculation agrees quite well with the experimental data⁽³⁷⁾ except for the maxima being too high and shifted towards lower momentum transfers.

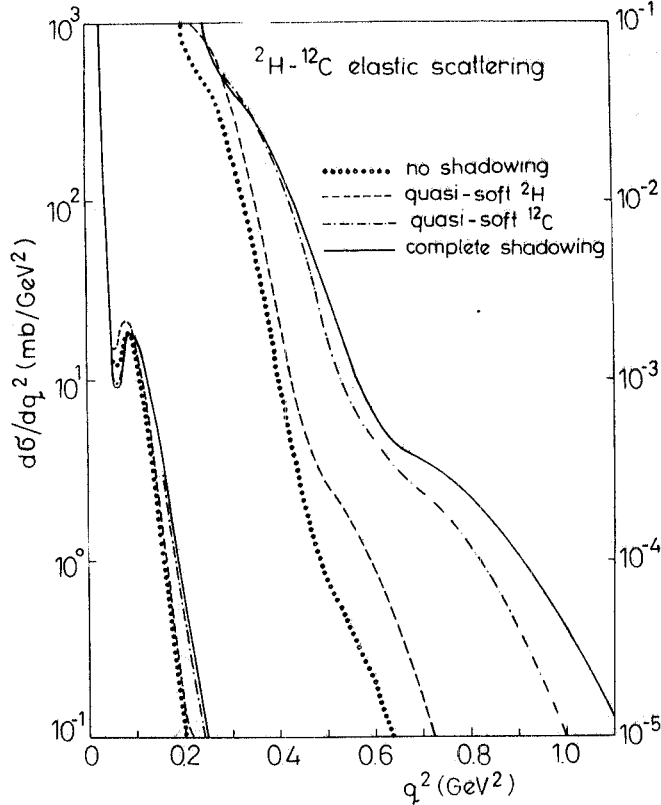


FIG. 14 - The differential cross-section of ${}^2\text{H}-{}^{12}\text{C}$ elastic scattering in the Glauber model, corresponding to various approximations to the nuclear profile. The no-shadowing, quasi-soft projectile and quasi-soft target approximations are compared with the complete multiple scattering calculation. The Gaussian nuclear radii are $R_2 = 2.28$ fm, $R_{12} = 1.93$ fm. The nucleon parameters are appropriate for the 650 MeV/n collision: $\sigma = 39.3$ mb, $\alpha = -0.4$, $a = 3.4$ GeV $^{-2}$.

In Eq. (55) we made use of the probabilistic interpretation of the nuclear profile. The first term in the right-hand side represents the probability that none of the colliding nuclei is virtually excited, the second term corresponds to a situation when the target becomes excited but the projectile permanently remains in its ground state, the third term describes the opposite case, and the last term gives probability of a simultaneous excitation of the two nuclei. Summing up those four contributions one obtains:

The size of quasi-elastic shadowing and hence the differences between Eqs. (48, 51, 52) and the complete multiple-scattering calculation, will, in general, depend on the correlation structure of colliding nuclei⁽²²⁾. The strong correlations among nucleons would increase the chance for virtual excitations in colliding nuclei. In the independent-particle model (20) the nuclear correlations originate from the c. m. constraint which is mostly important for light nuclei. Also the short-range correlations are most effective for these nuclei. Therefore, when $B > A$, it should be useful, though numerically more time-consuming, to apply the approximation of "rigid" or "quasi-soft" nucleus rather than to the lighter projectile⁽³⁰⁾. The example shown in Fig. 14 confirms this conjecture.

In the approximations of the quasi-soft or rigid projectile as well as in their analogues for the target nucleus, the colliding nuclei are treated on an unequal footing. This is in contrast to the symmetry originally present in the complete multiple-scattering formula (13). This drawback may, however, be remedied by writing the nucleus-nucleus profile down as follows⁽⁴⁰⁾:

$$\begin{aligned} \Gamma^{\text{sym}} = & \Gamma^{\text{NS}} \\ & + (\Gamma^{\text{RP}} - \Gamma^{\text{NS}}) [1 - (\Gamma^{\text{RT}} - \Gamma^{\text{NS}})] \\ & + (\Gamma^{\text{RT}} - \Gamma^{\text{NS}}) [1 - (\Gamma^{\text{RP}} - \Gamma^{\text{NS}})] \\ & + (\Gamma^{\text{RP}} - \Gamma^{\text{NS}}) (\Gamma^{\text{RT}} - \Gamma^{\text{NS}}). \end{aligned} \quad (55)$$

$$\Gamma^{\text{sym}} = \Gamma^{\text{RP}} + \Gamma^{\text{RT}} - \Gamma^{\text{NS}} - (\Gamma^{\text{RP}} - \Gamma^{\text{NS}})(\Gamma^{\text{RT}} - \Gamma^{\text{NS}}), \quad (56)$$

We wish to point out that the profile of a rigid target Γ^{RT} can be cast in a form which is convenient for numerical calculations. For large B one may write:

$$\begin{aligned} \Gamma^{\text{RT}} &= 1 - \langle 0_A | \prod_{j=1}^A \left\{ \prod_{k=1}^B \left[1 - \langle 0_B | \gamma_{jk}(\vec{b} + \vec{s}_{jA} - \vec{s}_{kB}) | 0_B \rangle \right] \right\} | 0_A \rangle \approx \\ &\approx 1 - \langle 0_A | \exp \left[-B \sum_{j=1}^A \langle 0_B | \gamma_{j1}(\vec{b} + \vec{s}_{jA} - \vec{s}_{1B}) | 0_B \rangle \right] | 0_A \rangle \approx \\ &\approx 1 - \langle 0_A | \prod_{k=1}^B \left[1 - \sum_{j=1}^A \langle 0_B | \gamma_{j1}(\vec{b} + \vec{s}_{jA} - \vec{s}_{1B}) | 0_B \rangle \right] | 0_A \rangle. \end{aligned} \quad (57)$$

The second line of Eq. (57) constitutes an exponential approximation to both the first and third lines. The second and third lines in Eq. (57) can be identified as the dominating terms in the so-called "swarm projectile model" of Faldt and Hulthage⁽⁴²⁾. Eq. (57) indicates then that this model is closely related to the approximations based upon the concept of quasi-elastic shadowing. Indeed, a numerical calculation⁽⁴⁰⁾ shows that for $B \gg 10$ the difference between the rigid-target and the swarm-projectile approximations is negligible.

The symmetric formula (56) (compare also Ref. (41)) is the main result of the present approach. The agreement with the complete multiple-scattering calculation is quite good except for very large momentum transfers where some shadowing still seems to be missing - see Figs. 15 and 16. It should be stressed that the profiles occurring in Eq. (56) are those of the rigid projectile (RP) and of the rigid target (RT). They must not be replaced with quasi-soft profiles since this would lead to a double-counting of excitations; the example shown in Fig. 16 makes this point clear.

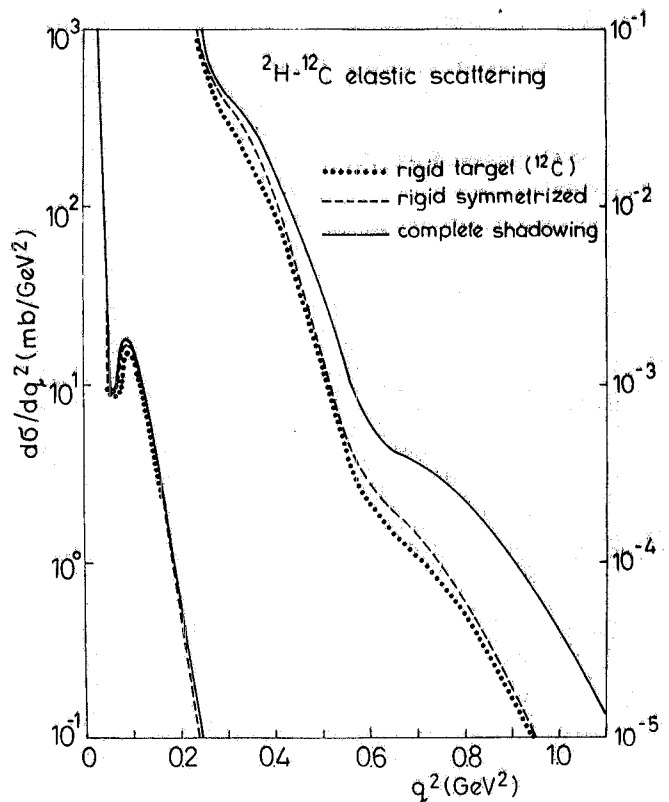


FIG. 15 - The differential cross-section of $^2\text{H}-^{12}\text{C}$ elastic scattering in the Glauber model, corresponding to various approximations to the nuclear profile. The rigid target approximation (Eq. (57)) and the symmetric formula (56) are compared with the complete multiple-scattering calculation. Same parameters as in Fig. 14.

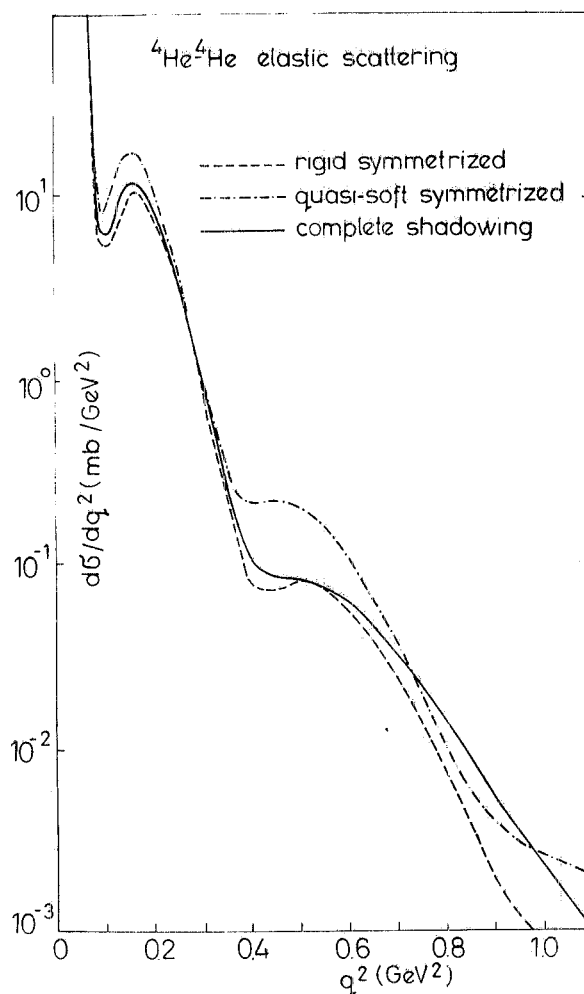
5. - SUMMARY.

We have described two approaches to multiple scattering in nucleus-nucleus collisions. The first one has been the eikonal Glauber model that is appropriate for high-energy collisions. The second approach, grounded upon the construction of a microscopic optical potential, makes possible to extend the description of multiple scattering towards lower energies.

The main calculational difficulty in both approaches is the evaluation of the nucleus-nucleus profile function. The profile is expressed in terms of the nuclear densities and of the nucleon-nucleon scattering amplitudes. Various perturbative techniques have been presented. They differ by the quantity which is being expanded according to the number of elementary amplitudes: the nuclear profile itself, the optical potential or the eikonal phase-shift.

Finally, we have discussed a relatively novel method which is based on the concept of quasi-elastic shadowing arising from virtual nuclear excitations. Useful approximations to the complete multiple-scattering calculation have been obtained by partially neglecting the intermediate excitations of the colliding nuclei.

FIG. 16 - The differential cross-section of ${}^4\text{He}-{}^4\text{He}$ elastic scattering in the Glauber model, corresponding to the nuclear profile. The symmetric formula (56) with the rigid profiles and its analogue with the quasi-soft profiles are compared with the complete multiple-scattering calculation. Same parameters as in Fig. 11.



ACKNOWLEDGEMENT.

Most of the numerical results included in this paper have been obtained in a collaboration with Dr. R. Dymarz. Special thanks go to Dr. A. Kobos for discussions regarding the manuscript.

It is a pleasure to thank Profs. P. Picchi, A. Reale and R. Scrimaglio for the warm hospitality at the Laboratori Nazionali dell'INFN at Frascati. These lecture notes are a part of author's activity at the Laboratori Nazionali di Frascati in 1979.

REFERENCES.

- (1) - R. A. Broglia and A. Winther, Phys. Rep. 4C, 153 (1972).
- (2) - R. A. Broglia, S. Landowne, R. A. Malfliet, V. Rostokin and A. Winther, Phys. Rep. 11C, 1 (1974).
- (3) - T. Koeling and R. A. Malfliet, Phys. Rep. 22C, 182 (1975).
- (4) - J. Knoll and R. Schaeffer, Ann. of Phys. 97, 307 (1976).
- (5) - G. Moliere, Z. Naturf. 2A, 133 (1947).
- (6) - R. J. Glauber, in: Lectures in Theoretical Physics, ed. by W. E. Brittin and L. C. Dunham (Interscience, 1959), Vol. 1, p. 315.
- (7) - T. W. Donnelly, J. Dubach and J. D. Walecka, Nuclear Phys. 232A, 355 (1974).
- (8) - W. Czyz and L. C. Maximon, Ann. of Phys. 52, 59 (1969).
- (9) - L. L. Foldy and J. D. Walecka, Ann. of Phys. 54, 447 (1969).
- (10) - W. E. Frahn, Ann. of Phys. 72, 524 (1972).
- (11) - W. Czyz, L. Lesniak and H. Wołek, Nucler Phys. B19, 125 (1970).
- (12) - R. J. Glauber, in: High Energy Physics and Nuclear Structure, ed. by S. Devons (Plenum, 1970), p. 207; W. Czyz, Adv. Nuclear Phys. 4, 61 (1971).
- (13) - S. Gartenhaus and C. Schwartz, Phys. Rev. 108, 482 (1957).
- (14) - R. Dymarz and A. Małecki, Phys. Letters 66B, 413 (1977).
- (15) - K. M. Watson, Phys. Rev. 89, 575 (1953); 105, 1388 (1957); M. L. Goldberger and K. M. Watson, in: Collision Theory (Wiley, 1964), p. 749.
- (16) - J. M. Eisenberg, Ann. of Phys. 71, 542 (1972).
- (17) - A. Małecki, IFJ Raport No. 1048/PH, Krakow (1979); R. Dymarz and A. Małecki, to be published.
- (18) - R. L. Sugar and R. Blankenbecler, Phys. Rev. 183, 1387 (1969).
- (19) - S. J. Wallace, Phys. Rev. C12, 179 (1975).
- (20) - R. Dymarz and A. Małecki, Phys. Letters 83B, 15 (1979); 86B, 427 (1979).
- (21) - A. Małecki and L. Satta, Lett. Nuovo Cimento 21, 457 (1978).
- (22) - R. Dymarz and A. Małecki, Journ. de Phys. Lettres 40, 425 (1979).
- (23) - A. Vitturi and F. Zardi, Lett. Nuovo Cimento 20, 640 (1977).
- (24) - J. Berger et al., in: Proceedings 7th Intern. Conf. on High Energy Physics and Nuclear Structure, Zurich, 1977, Abstract Vol., p. 160.
- (25) - W. Czyz and L. C. Maximon, Ann. of Phys. 60, 484 (1970).
- (26) - D. V. Bugg et al., Phys. Rev. 146, 980 (1966); T. J. Devlin et al., Phys. Rev. D8, 136 (1973).
- (27) - G. K. Varma, Nuclear Phys. A294, 475 (1978).
- (28) - V. Franco and G. K. Varma, Phys. Rev. C15, 1375 (1977).
- (29) - V. Franco and G. K. Varma, Phys. Rev. C18, 349 (1978).
- (30) - R. Dymarz, A. Małecki, K. Gluski and P. Picchi, Lett. Nuovo Cimento 24, 1 (1979); E25, 479 (1979).
- (31) - W. L. Wang and R. G. Lipes, Phys. Rev. C9, 814 (1974).
- (32) - P. S. Fishbane and J. S. Trefil, Phys. Rev. D10, 3128 (1974).
- (33) - S. Barshay, C. B. Dover and J. P. Vary, Phys. Rev. C11, 360 (1975).
- (34) - J. Höfner, K. Schäfer and B. Schürmann, Phys. Rev. C12, 1888 (1975).
- (35) - V. Franco, Phys. Letters 61B, 444 (1976); 64B, 13 (1976).
- (36) - A. Małecki, K. Gluski and P. Picchi, in: Proceedings 7th Intern. Conf. on High Energy Physics and Nuclear Structure, Zurich, 1977, Abstract Vol., p. 178.
- (37) - G. D. Alkhazov et al., Nuclear Phys. A280, 365 (1977).
- (38) - R. D. Viollier and E. Turtschi, CERN Report TH-2529 (1978).
- (39) - G. Igo, in: High Energy Physics and Nuclear Structure, ed. by D. E. Nagle et al. (AIP, New York, 1975), p. 63.
- (40) - R. Dymarz and A. Małecki, to be published.
- (41) - A. Smida, Thesis, Moscow 1979.
- (42) - G. Faldt and I. Hulthage, Nuclear Phys. A316, 253 (1979).